

RSC Advances



This is an *Accepted Manuscript*, which has been through the Royal Society of Chemistry peer review process and has been accepted for publication.

Accepted Manuscripts are published online shortly after acceptance, before technical editing, formatting and proof reading. Using this free service, authors can make their results available to the community, in citable form, before we publish the edited article. This *Accepted Manuscript* will be replaced by the edited, formatted and paginated article as soon as this is available.

You can find more information about *Accepted Manuscripts* in the [Information for Authors](#).

Please note that technical editing may introduce minor changes to the text and/or graphics, which may alter content. The journal's standard [Terms & Conditions](#) and the [Ethical guidelines](#) still apply. In no event shall the Royal Society of Chemistry be held responsible for any errors or omissions in this *Accepted Manuscript* or any consequences arising from the use of any information it contains.

ARTICLE

Aggregation-Induced Emission Block Copolymers Based on Ring-Opening Metathesis Polymerization

Cite this: DOI: 10.1039/x0xx00000x

Yuming Zhao, Ying Wu, Guowei Yan, Ke Zhang*

Received 00th January 2012,
Accepted 00th January 2012

DOI: 10.1039/x0xx00000x

www.rsc.org/

The aggregation-induced emission (AIE) amphiphilic block copolymers were developed based on the living ring-opening metathesis polymerization for the first time. By virtue of the block copolymer self-assembly in selective solvents, water soluble fluorescent nano-objects were then prepared with various structures including spherical micelles, cylindrical micelles, and vesicles. This method represents a facile and efficient way to prepare the well-defined AIE polymers and the varied fluorescent nano-objects with controlled structures and functionalities thereof.

Introduction

Aggregation-induced emission (AIE) materials have received considerable attention¹⁻⁴ since the AIE term was coined in Tang's group in 2001⁵. In contrast to the notorious aggregation-caused fluorescence quenching (ACQ) characteristics of traditional fluorophores, AIE fluorogens endows luminescent materials with strong fluorescence emission in aggregate formation. This makes it play a very important role in a variety of practical applications such as fluorescence sensors^{6,7}, biological probes^{8,9}, and optoelectronic applications¹⁰⁻¹². To date, varied AIE fluorogens have been developed including tetraphenylethene (TPE)¹³, silole^{5,14}, and distyrylanthracene¹⁵, in which the restricted intramolecular rotation has been suggested as the mechanism for their AIE phenomenon.^{1,2} By integrating the AIE fluorogens into polymer chains as side, main-chain, or end groups, AIE polymeric materials could be conveniently produced. Thanks to the good solubility, processability, and high AIE efficiency, the exploration of AIE polymers with varied macromolecular structures and functionalities has become one of the critical developing directions in this research field.^{3,4}

The known synthetic methods for AIE polymers can be generalized into two categories including step and chain polymerizations. The step polymerization techniques usually produce branched or ill-defined linear AIE polymers with relatively lower molecular weight and broad polydispersity index (PDI). The resultant polymers generally contain the fluorogens inside of polymer main-chains.^{6,16-23} The chain polymerization methods, however, typically yield linear AIE polymers with higher molecular weight. The AIE fluorogens are usually designed as side groups in this case.²⁴⁻³⁹ Especially when living chain polymerization techniques were used, the well-defined linear AIE polymers were produced with controlled molecular weight and narrow PDI.³¹⁻³⁵ To date, the controlled free radical polymerization methods including atom transfer radical polymerization (ATRP)³¹⁻³³ and reversible addition-fragmentation chain transfer polymerization (RAFT)³⁴⁻

³⁹ have already been applied to prepare well-defined AIE polymers. The corresponding nanomaterials from the resultant well-defined AIE polymers have demonstrated the varied applications as fluorescence sensors and biological imaging probes.³¹⁻³⁹

As far as we know, ring-opening metathesis polymerization (ROMP)⁴⁰, as one of the most powerful controlled polymerization methods, has never been used to produce AIE polymers. Recently, ROMP has been developed to produce a variety of well-defined polymers at very mild conditions such as at room temperature, in a few minutes, and even opening in air.^{41,42} More importantly, the monomer could be consumed with a quantitative conversion during ROMP, while the resultant polymers still keep the narrow PDI and the active propagating terminals for further chain extension. This makes it a convenient and powerful method to prepare block copolymers since the precursor macroinitiators do not need to be purified and isolated. By directly adding the second monomer into the polymerization mixture after consuming the first one, the block copolymers could be conveniently produced. In addition, ROMP could produce polymers with a double bond in each repeat unit, which provides the valuable reactive sites for further post-functionalizing the polymers. Herein, we explored the ROMP to produce AIE polymers for the first time. Figure 1 includes our design and synthetic procedure, in which the preparation of AIE amphiphilic diblock copolymers was used as an example to demonstrate our concept. The norbornene based monomers **M1** and **M2** were designed with a TPE AIE fluorogen as side group and a PEG as side chain respectively. Using the third generation Grubbs' catalyst (**G3**) as initiator, a series of well-defined AIE diblock copolymers of poly(**M1**)-*b*-poly(**M2**) were produced in less than one hour at room temperature. In addition, by virtue of their self-assembly in selective solvents, water soluble fluorescent nano-objects were produced with varied structures including spherical micelles, cylindrical micelles, and vesicles. Since the biocompatible PEG was designed on the surface of these novel nano-objects, they should have a potential application as the biological imaging probes.

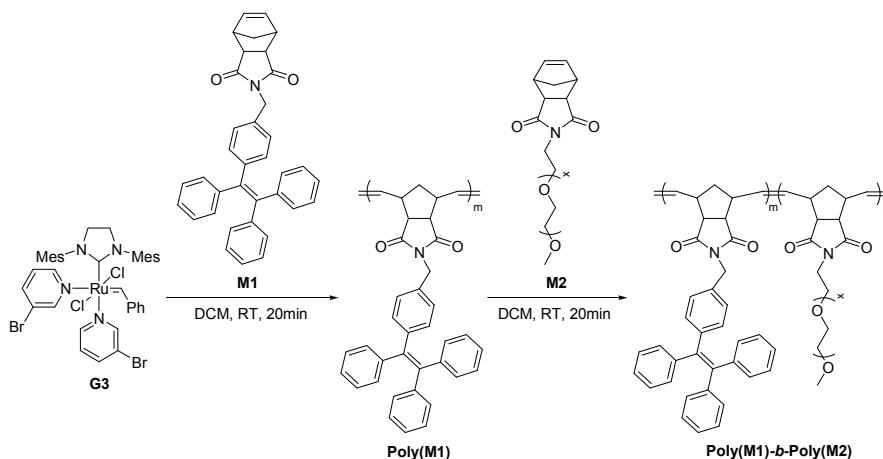


Figure 1. The preparation of AIE amphiphilic diblock copolymer of poly(**M1**)-*b*-poly(**M2**).

Experimental

Materials

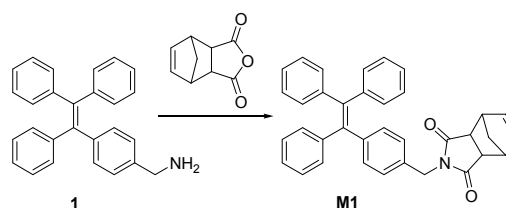
4-Methylbenzophenone, diphenylmethane, *n*-butyllithium (*n*-BuLi, 2.4 M in hexane), ammonium chloride (NH₄Cl), *p*-toluenesulfonic acid (*p*-TSA), *N*-bromosuccinimide (NBS), benzoyl peroxide (BPO), *N*-potassium phthalimide, hydrazine hydrate (80 wt.% solution in H₂O) (N₂H₄), *cis*-5-norbornene-*exo*-2,3-dicarboxylic anhydride, polyethylene glycol monomethylether (*M_n*=750, PEG₇₅₀-OH), methanesulfonyl chloride (MsCl), triethylamine (TEA), sodium azide (NaN₃), triphenylphosphine (P(Ph)₃), sodium hydroxide (NaOH), potassium hydroxide (KOH), sodium chloride (NaCl), anhydrous magnesium sulfate (MgSO₄), carbon tetrachloride (CCl₄), dichloromethane (DCM), tetrahydrofuran (THF), methanol, ethanol, *N,N*-dimethylformamide (DMF), toluene, petroleum ether, ethyl acetate, chloroform (CHCl₃), 1,4-dioxane, diethyl ether, ethyl vinyl ether (EVE), 3-bromo-pyridine, second generation Grubbs' catalyst (**G2**) were purchased as reagent grade from Alfa Aesar, Aldrich, Acros, J&K Chemical, or Beijing Chemical Reagent Co. and used as received unless otherwise noted. The third generation Grubbs' catalyst (**G3**) (dichloro-di-(3-bromopyridino)-*N,N'*-dimethylenoimidazolino-Ru=CHPh) was prepared according to the previously reported procedure.⁴³ TEA was dried over KOH. For making dry solvents: DCM was refluxed over calcium hydride; THF and toluene were distilled from sodium/benzophenone.

Characterization

¹H-NMR and ¹³C NMR spectra were recorded on a Bruker Avance 400 spectrometer at room temperature. Fluorescence spectra were recorded using a Cary Eclipse fluorescence spectrophotometer. Fluorescence images of self-assemblies were taken on an Olympus IX71 fluorescence microscope. Fluorescence quantum yields (Φ_f) were measured on a Hamamatsu C11347-11 quantum yield spectrometer. Gel permeation chromatography (GPC) was performed using four Waters Styragel columns (HT 2, HT 3, HT 4, and HT 5), a Waters 1515 isocratic HPLC pump, and a Waters 2414 RI detector. THF was used as the eluent at a flow rate of 1.0 mL/min. Polystyrene standards were used for the calibration.

Transmission electron microscopy (TEM) images were obtained using a JEM 1011 instrument operated at an accelerating voltage of 80 kV. The images were recorded by a digital camera. Solution samples (10–15 μ L) were dropped onto carbon-coated copper grids for TEM observation. FT-IR spectra were recorded on a Thermo Nicolet Avatar-330 Spectrometer at room temperature. Matrix-assisted laser desorption/ionization Fourier transform mass spectrometry (MALDI FTMS) experiments were performed on an Bruker Solarix MALDI Fourier transform mass spectrometer equipped with a 9.4-T actively shielded superconducting magnet. A 337 nm nitrogen laser was used for ionization/desorption. Matrix-assisted laser desorption/ionization time of flight (MALDI-TOF) mass spectrum was recorded on a Bruker Biflex III MALDI-TOF mass spectrometer equipped with a 337 nm nitrogen laser.

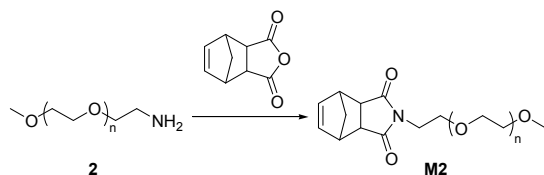
Preparation of **M1**



The synthesis of Compound **1** was detailed in Supporting Information. Compound **1** (2.48 g, 6.87 mmol), *cis*-5-norbornene-*exo*-2,3-dicarboxylic anhydride (1.69 g, 10.30 mmol), and TEA (0.07 g, 0.69 mmol) were mixed with 50 mL toluene in a 150 mL round-bottom flask fitted with a Dean-Stark apparatus. After refluxing the reaction for around 12 h, the reaction solution was cooled and concentrated. The crude product was purified by a silica gel column with DCM/CH₃OH (10/1, v/v) as eluent to provide the white solid product **M1** (2.67 g, 76.72 % yield). ¹H-NMR (CDCl₃), δ (ppm): 7.13–7.03 (m, 11H), 7.03–6.91 (m, 8H), 6.28 (s, 2H), 4.52 (s, 2H), 3.23 (s, 2H), 2.67 (s, 2H), 1.42–1.32 (m, 1H), 1.01–0.91 (m, 1H). ¹³C NMR (CDCl₃), δ (ppm): 177.60, 143.46, 141.20, 140.38,

137.97, 133.88, 131.51, 131.24, 128.11, 127.61, 126.42, 47.70, 45.34, 42.56, 42.03. HRMS (MALDI) m/z calculated for $C_{36}H_{29}NO_2$ [M^+] 507.2198, found 507.2193. FT-IR spectrum was shown in Supporting Information as Figure S1.

Preparation of M2



The synthesis of PEG₇₅₀-NH₂ (**2**) was detailed in Supporting Information. PEG₇₅₀-NH₂ (3.00 g, 4.00 mmol), cis-5-norbornene-exo-2,3-dicarboxylic anhydride (0.79 g, 4.80 mmol), and TEA (0.04 g, 0.40 mmol) were mixed with 50 mL toluene in a 150 mL round-bottom flask fitted with a Dean-Stark apparatus. After refluxing the reaction for around 12 h, the reaction solution was cooled and concentrated. The crude product was purified by a silica gel column with DCM/CH₃OH (20/1, v/v) as eluent to provide the white semisolid product **M2** (1.33 g, 37.15 % yield). ¹H-NMR (CDCl₃), δ (ppm): 6.28 (s, 2H), 3.70-3.59 (m, 64H), 3.38 (s, 3H), 3.26 (s, 2H), 2.67 (s, 2H), 1.52-1.45 (m, 1H), 1.39-1.34 (m, 1H). ¹³C NMR (CDCl₃), δ (ppm): 177.97, 137.83, 76.68, 71.94, 70.57, 69.87, 66.87, 59.03, 47.81, 45.27, 42.72, 37.73. FT-IR and MOLDI-TOF MS spectra were shown in Supporting Information as Figure S2 and S3 respectively.

Preparation of poly(M1)-*b*-poly(M2) diblock copolymers

A general ROMP procedure was demonstrated by the preparation of poly(**M1**)₃₀₀-*b*-poly(**M2**)₁₀. **G3** (1.2 mg, 1.31×10^{-3} mmol), **M1** (200 mg, 0.39 mmol) and **M2** (12 mg, 0.013 mmol) were separately dissolved in a 25 mL Schlenk tube with 1 mL DCM. After degassing through three freeze-evacuate-thaw cycles, the **M1** solution was added all at once to the catalyst **G3** solution at room temperature under N₂ while stirring vigorously. After reacting for 20 min, the second monomer **M2** solution was added to the above system under the same conditions. After stirring at room temperature for another 20 min, the reaction was quenched by addition of 0.5 mL EVE. The mixture was concentrated and then precipitated in diethyl ether to obtain the diblock copolymer of poly(**M1**)₃₀₀-*b*-poly(**M2**)₁₀. FT-IR spectra of poly(**M1**)₃₀₀ and poly(**M1**)₃₀₀-*b*-poly(**M2**)₁₀ were shown in Supporting Information as Figure S4 A and B respectively.

Critical Micelle Concentration

The critical micelle concentration (CMC) was determined by fluorescence spectroscopy. A stock solution of poly(**M1**)-*b*-poly(**M2**) was prepared with a concentration of 0.1 mg/mL. Ten diluted solutions were then prepared from the stock with different polymer concentration and a minimum of 1×10^{-5} mg/mL. After that, fluorescence spectrum was recorded for each sample. The intensities of the peak at 480 nm were then

collected to plot with the corresponding polymer concentrations. The CMC was finally determined from the curve of fluorescence intensity vs. polymer concentration, quantifying by the polymer concentration at the intersection between the plateau and the tangent of the increase of fluorescence intensity.

Self-assembly of poly(M1)-*b*-poly(M2) diblock copolymers

A general procedure: 0.8 mL water was added dropwise into 0.2 mL poly(**M1**)-*b*-poly(**M2**) THF or dioxane solution (10 mg/mL) within 10 min by syringe under vigorous stirring. After 12 h, the self-assemblies were characterized.

Results and Discussion

Synthesis of monomers

The norbornene based monomers of **M1** and **M2** were prepared by reacting cis-5-norbornene-exo-2,3-dicarboxylic anhydride with 1-[(4-aminomethyl) phenyl]-1,2,2-triphenylethene (**1** in Experimental) and PEG₇₅₀-NH₂ (**2** in Experimental), respectively. The detailed synthesis process was shown in Experimental. The ¹H-NMR spectra and the related peak assignments are shown in Figure 2 A and B for **M1** and **M2** respectively, which clearly indicated the successful preparation of the norbornene based monomers.

Preparation of poly(M1)-*b*-poly(M2) diblock copolymers

ROMP was selected to sequentially polymerize **M1** and **M2** for the formation of well-defined poly(**M1**)-*b*-poly(**M2**) diblock copolymers (Figure 1), in which **G3** was used as the initiator. By this method, the block ratio could be conveniently controlled by the initial molar ratio between **M1** and **M2**. The preparation of poly(**M1**)₃₀₀-*b*-poly(**M2**)₁₀ was detailed as an example to demonstrate the ROMP living characteristics for producing the well-defined poly(**M1**)-*b*-poly(**M2**) diblock copolymers. Using $[M1]_0/[G3]_0 = 300/1$, the poly(**M1**)₃₀₀ was obtained at room temperature in 20 min with $[M1]_0 = 0.2$ M in DCM. By subsequently adding **M2** in-situ to extend the polymer chain of poly(**M1**)₃₀₀ with $[M1]_0/[M2]_0 = 300/10$, the diblock copolymer of poly(**M1**)₃₀₀-*b*-poly(**M2**)₁₀ was produced in another 20 min at room temperature. After the polymerization, EVE was then used to detach Ru catalyst from the polymer chain end, resulting the metal free poly(**M1**)₃₀₀-*b*-poly(**M2**)₁₀.

Figure 2C shows the ¹H-NMR spectrum of an aliquot of poly(**M1**)₃₀₀ polymerization solution without purification after the first polymerization step. The complete disappearance of the peak at 6.28 ppm (peak a in Figure 2A) ascribed to -CH=CH- in **M1** was observed and new broad peaks appeared at 5.34-5.82 ppm (peak a' in Figure 2C), belonging to -CH=CH- in poly(**M1**). This indicated that the polymerization was carried out successfully with a quantitative **M1** conversion. Figure 3A (black) shows the corresponding GPC curve with a symmetric and monomodal peak that corresponds to $M_n = 132600$ g/mol and PDI = 1.06 (Table 1, Run 1).

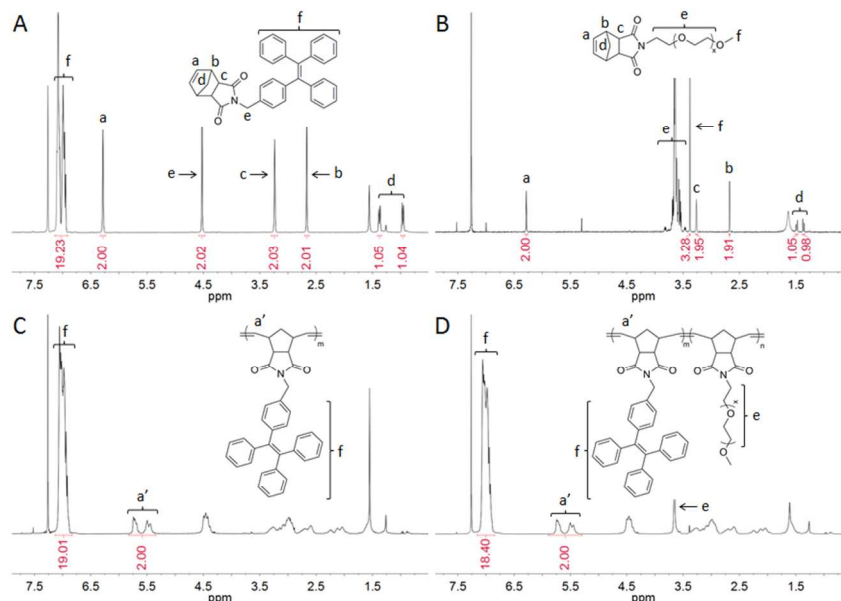


Figure 2. ¹H-NMR spectra of norbornene based monomers **M1** (A) and **M2** (B) and the resultant homopolymer poly(**M1**)₃₀₀ (C) and diblock copolymer poly(**M1**)₃₀₀-*b*-poly(**M2**)₁₀ (D).

Table 1. Synthesis and characterization of poly(**M1**) macroinitiators and the corresponding poly(**M1**)-*b*-poly(**M2**) diblock copolymers.

Run ^{a)}	Polymer	Feed ratio	$M_{n,theory}$ ^{d)}	$M_{n,GPC}$ ^{e)}	PDI ^{e)}
1	poly(M1) ₃₀₀	300:1 ^{b)}	152100	132600	1.06
2	poly(M1) ₃₀₀ - <i>b</i> -poly(M2) ₁₀	10:1 ^{c)}	161100	135800	1.07
3	poly(M1) ₁₀₀	100:1 ^{b)}	50700	43400	1.03
4	poly(M1) ₁₀₀ - <i>b</i> -poly(M2) ₁₀	10:1 ^{c)}	59700	45100	1.03
5	poly(M1) ₅₀	50:1 ^{b)}	25300	19200	1.04
6	poly(M1) ₅₀ - <i>b</i> -poly(M2) ₁₀	10:1 ^{c)}	34300	23600	1.03

^{a)} ROMP polymerizations were all performed at room temperature in DCM. ^{b)} [**M1**]₀/[**G3**]₀ employed for the preparation of poly(**M1**) macroinitiators. ^{c)} [**M2**]₀/[poly(**M1**)]₀ employed for the preparation of poly(**M1**)-*b*-poly(**M2**) diblock copolymers, which theoretically equaled to [**M2**]₀/[**G3**]₀ in the used ROMP approach. ^{d)} Calculated from the feed ratio. ^{e)} Calculated from GPC, in which THF was used as eluent and polystyrene standards were used for calibration.

Figure 2D shows the ¹H-NMR spectrum of an aliquot of poly(**M1**)₃₀₀-*b*-poly(**M2**)₁₀ polymerization solution without purification after the second polymerization step. Compared to that of **M2** (Figure 2B), the peak at 6.28 ppm (peak a in Figure 2B) ascribed to -CH=CH- in **M2** was completely disappeared. In addition, a new peak was clearly observed at 3.65 ppm assigned to -CH₂CH₂O- of poly(**M2**) block, compared to that of poly(**M1**)₃₀₀ (Figure 2C). This indicated the polymerization was carried out successfully with a quantitative **M2** conversion. Figure 3A (red) shows the corresponding GPC curve. Compared to that (black curve) of the precursor poly(**M1**)₃₀₀, the symmetric and monomodal peak shape was preserved but the peak position completely shift to higher molecular weight direction. The corresponding M_n and PDI was integrated as 135800 g/mol and 1.07 (Table 1, Run 2). This clearly indicated the successful chain extension of poly(**M1**) and the formation of well-defined poly(**M1**)₃₀₀-*b*-poly(**M2**)₁₀.

Taking advantage of the same procedure, poly(**M1**)₁₀₀-*b*-poly(**M2**)₁₀ and poly(**M1**)₅₀-*b*-poly(**M2**)₁₀ were produced simply by controlling [**M1**]₀/[**M2**]₀/[**G3**]₀ as 100/10/1 and 50/10/1. The corresponding GPC curves were shown in Figure 3 B and C, in which the symmetric and monomodal peaks were observed for all cases. Compared to those of precursors poly(**M1**)₁₀₀ and poly(**M1**)₅₀, the peak position for the resultant poly(**M1**)₁₀₀-*b*-poly(**M2**)₁₀ and poly(**M1**)₅₀-*b*-poly(**M2**)₁₀ completely shifted to high molecular weight direction. The corresponding M_n and PDI was calculated as 45100 g/mol and 1.03 for poly(**M1**)₁₀₀-*b*-poly(**M2**)₁₀ (Table 1, Run 4) and as 23600 g/mol and 1.03 for poly(**M1**)₅₀-*b*-poly(**M2**)₁₀ (Table 1, Run 6).

Self-assembly of poly(**M1**)-*b*-poly(**M2**) and the AIE nano-objects thereof

The self-assembly behavior of this novel kind of AIE amphiphilic diblock copolymers was investigated in selective solvents. A general

self-assembly procedure was demonstrated as follows. Poly(M1)-*b*-poly(M2) (2 mg) was dissolved in 0.2 mL THF or dioxane (only for poly(M1)₃₀₀-*b*-poly(M2)₁₀), which are the good solvents for both blocks. A selective solvent water (0.8 mL) was then added slowly under vigorous stirring to induce the self-assembly. Since water is a non-solvent for poly(M1) but a good solvent for poly(M2), the self-assemblies were obtained in this situation with poly(M1) block as the aggregating part and poly(M2) as the dispersing part. Taking advantage of this method, the structures of the resultant self-assemblies could be manipulated conveniently by changing the block ratio of poly(M1)-*b*-poly(M2). Due to the AIE property of poly(M1) block, the self-assemblies with varied structures were all endowed with strong fluorescent characteristics.

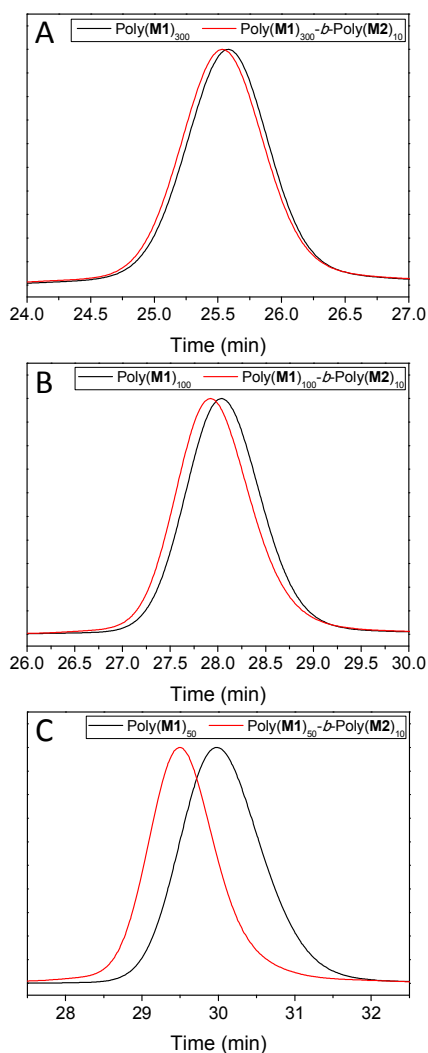


Figure 3. GPC curves of (A) poly(M1)₃₀₀ (black) and the resultant poly(M1)₃₀₀-*b*-poly(M2)₁₀ (red), (B) poly(M1)₁₀₀ (black) and the resultant poly(M1)₁₀₀-*b*-poly(M2)₁₀ (red), and (C) poly(M1)₅₀ (black) and the resultant poly(M1)₅₀-*b*-poly(M2)₁₀ (red).

Figure 4A shows the TEM image of self-assemblies from poly(M1)₅₀-*b*-poly(M2)₁₀, in which the spherical micelles were clearly observed with a diameter of ca. 25 nm. Figure 4B is the

corresponding fluorescence microscope image, where the fluorescent nanospheres were demonstrated. Figure 4C shows the picture of poly(M1)₅₀-*b*-poly(M2)₁₀ THF solution (left) and the micelle dispersion in mixed THF and water (*v/v* = 1/4) (right). Compared to the polymer solution, the micelle dispersion emitted the strong fluorescence indicating the poly(M1) was aggregated and formed the micelle core. The quantitative fluorescent characterization was recorded by fluorescence spectrophotometer. As shown in Figure 4D, no fluorescence emission peak was observed from the spectrum (black) of poly(M1)₅₀-*b*-poly(M2)₁₀ THF solution. A strong emission peak, however, was observed from the spectrum (red) for the resultant micelle dispersion in water with a peak position at 480 nm. The corresponding Φ_F was measured as 0.20.

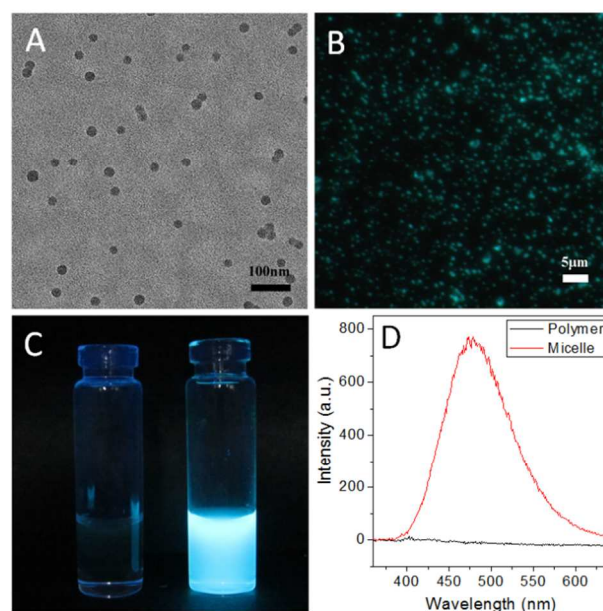


Figure 4. (A) TEM image and (B) fluorescence microscope image of the spherical micelles formed from poly(M1)₅₀-*b*-poly(M2)₁₀. (C) Pictures of the poly(M1)₅₀-*b*-poly(M2)₁₀ THF solution (left) and the resultant micelle dispersion in mixed THF and water (*v/v* = 1/4) (right). (D) Fluorescence spectra of the poly(M1)₅₀-*b*-poly(M2)₁₀ THF solution (black) and the resultant micelle dispersion in water (red).

Figure 5A shows the TEM image of cylindrical micelles formed from poly(M1)₁₀₀-*b*-poly(M2)₁₀, in which the cylinder diameter was measured as ca. 38 nm. Figure 5B shows the corresponding fluorescence microscope image. Different from the poly(M1)₁₀₀-*b*-poly(M2)₁₀ THF solution (Figure 5C left), the cylindrical micelle dispersion emitted the strong fluorescence in mixed THF and water (*v/v* = 1/4) (Figure 5C right). This is again demonstrated by fluorescence spectrum. As shown in Figure 5D, no emission signal was observed from the curve (black) of poly(M1)₁₀₀-*b*-poly(M2)₁₀ THF solution. The strong emission peak, however, was observed from the curve (red) of the resultant cylindrical micelle dispersion in water with a peak position at 480 nm. The corresponding Φ_F was measured as 0.21.

Figure 6A shows the TEM image of the vesicles formed from poly(M1)₃₀₀-*b*-poly(M2)₁₀, where the outer diameter was measured

as ca. 106 nm and the inner cavity was clearly observed. Figure 6B shows the corresponding fluorescence microscope image. Different from the poly(M1)₃₀₀-*b*-poly(M2)₁₀ dioxane solution (Figure 6C left), the vesicle dispersion emitted a strong fluorescence in mixed dioxane and water (v/v = 1/4) (Figure 6C right). From the fluorescence spectra (Figure 6D), no emission peak was observed from the curve (black) of poly(M1)₃₀₀-*b*-poly(M2)₁₀ dioxane solution. A strong emission peak, however, was shown in the curve (red) of the resultant vesicle dispersion in water with a peak position at 480 nm. The corresponding Φ_F was measured as 0.22.

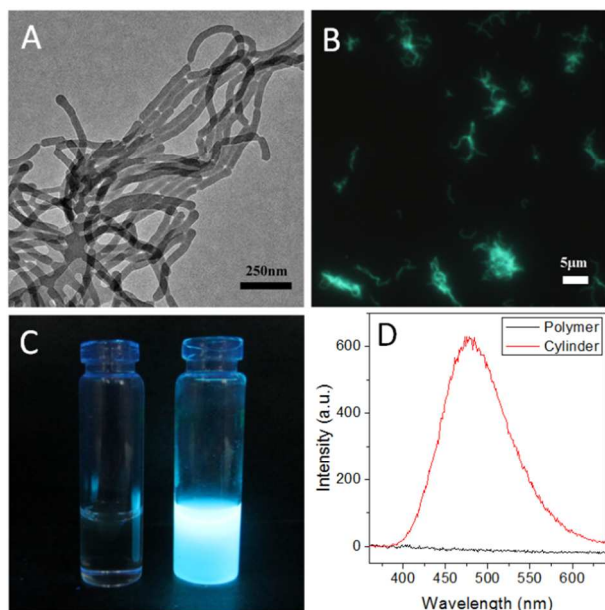


Figure 5. (A) TEM image and (B) fluorescence microscope image of the cylindrical micelles formed from poly(M1)₁₀₀-*b*-poly(M2)₁₀. (C) Pictures of the poly(M1)₁₀₀-*b*-poly(M2)₁₀ THF solution (left) and the resultant cylindrical micelle dispersion in mixed THF and water (v/v = 1/4) (right). (D) Fluorescence spectra of the poly(M1)₁₀₀-*b*-poly(M2)₁₀ THF solution (black) and the resultant cylindrical micelle dispersion in water (red).

Conclusively, the self-assembly morphologies from poly(M1)-*b*-poly(M2) could be manipulated from spheres, to rods, and further to vesicles simply by increasing the hydrophobic poly(M2) block content. This trend of self-assembly morphologies varied with poly(M1)-*b*-poly(M2) amphiphilicity consistently corresponds to that from other amphiphilic diblock copolymers reported in literature.⁴⁴⁻⁴⁶

In addition, the AIE characteristics provided a direct and convenient method for evaluating the CMC of poly(M1)-*b*-poly(M2) diblock copolymers. For doing this, fluorescence spectra were recorded for poly(M1)-*b*-poly(M2) solutions in a wide concentration range. The fluorescence intensities of AIE peak at 480 nm were then collected to plot with the corresponding polymer concentrations (Figure S5). Since the strong fluorescence was emitted only when block copolymer self-assemblies formed, The CMC could be determined from the curve of fluorescence intensity vs. polymer concentration, quantifying by the polymer concentration at the intersection between the plateau and the tangent of the increase of fluorescence intensity. By this method, the CMC was measured as 2.26×10^{-7} mol/L, 1.01×10^{-7} mol/L, and 3.92×10^{-8} mol/L for poly(M1)₅₀-*b*-poly(M2)₁₀ (Figure S5A), poly(M1)₁₀₀-*b*-poly(M2)₁₀

(Figure S5B), and poly(M1)₃₀₀-*b*-poly(M2)₁₀ (Figure S5C), respectively.

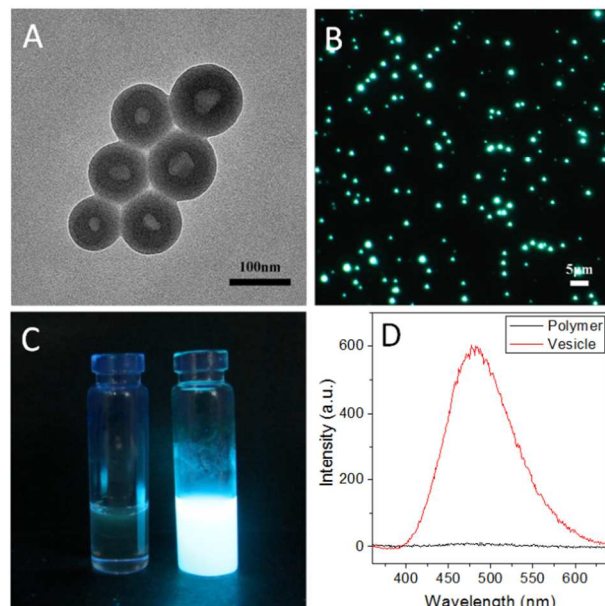


Figure 6. (A) TEM image and (B) fluorescence microscope image of the vesicles formed from poly(M1)₃₀₀-*b*-poly(M2)₁₀. (C) Pictures of the poly(M1)₃₀₀-*b*-poly(M2)₁₀ dioxane solution (left) and the resultant vesicle dispersion in mixed dioxane and water (v/v = 1/4) (right). (D) Fluorescence spectra of the poly(M1)₃₀₀-*b*-poly(M2)₁₀ dioxane solution (black) and the resultant vesicle dispersion in water (red).

Conclusions

ROMP has been demonstrated as a powerful tool to produce the well-defined amphiphilic AIE block copolymer of poly(M1)-*b*-poly(M2). The tetraphenylethene side group was designed in poly(M1) block to endow the copolymer hydrophobicity and AIE characteristic as well. The PEG side chains was introduced in poly(M2) block to fulfil its hydrophilicity. By self-assembling these novel AIE block copolymers in selective solvents, water soluble fluorescent nano-objects were conveniently prepared having an AIE hydrophobic poly(M1) aggregate part and a hydrophilic poly(M2) dispersing part. Simply by changing the block ratio of poly(M1)-*b*-poly(M2), the structures of the resultant nano-objects could be manipulated from spherical micelles to cylindrical micelles and to vesicles. As far as we know, this is the first time using ROMP to produce AIE block copolymers and varied fluorescent nano-objects thereof. The methods established and the AIE materials developed in this article should play an important role in polymer chemistry, fluorescence sensing, and biological and optoelectronic applications.

Acknowledgements

Generous support was primarily provided by Ministry of Science and Technology of China (2012CB933200 and 2014CB932200) and National Science Foundation of China (21090353 and 21374122). K. Z. thanks the *Bairen* project from The Chinese Academy of Sciences for support.

Notes and references

- † State Key Laboratory of Polymer Physics and Chemistry, Institute of Chemistry, The Chinese Academy of Sciences, Beijing 100190, China. Fax: +86-010-62559373; e-mail: kzhang@iccas.ac.cn
- 1 Y. Hong, J. W. Y. Lam and B. Z. Tang, *Chem. Commun.*, 2009, 4332-4353.
 - 2 Y. Hong, J. W. Y. Lam and B. Z. Tang, *Chem. Soc. Rev.*, 2011, **40**, 5361-5388.
 - 3 A. Qin, J. W. Y. Lam and B. Z. Tang, *Prog. Polym. Sci.*, 2012, **37**, 182-209.
 - 4 R. Hu, N. L. C. Leung and B. Z. Tang, *Chem. Soc. Rev.*, 2014, **43**, 4494-4562.
 - 5 J. Luo, Z. Xie, J. W. Y. Lam, L. Cheng, H. Chen, C. Qiu, H. S. Kwok, X. Zhan, Y. Liu, D. Zhu and B. Z. Tang, *Chem. Commun.*, 2001, 1740-1741.
 - 6 A. Qin, J. W. Y. Lam, L. Tang, C. K. W. Jim, H. Zhao, J. Sun and B. Z. Tang, *Macromolecules*, 2009, **42**, 1421-1424.
 - 7 X. Chen, X. Y. Shen, E. Guan, Y. Liu, A. Qin, J. Z. Sun and B. Z. Tang, *Chem. Commun.*, 2013, **49**, 1503-1505.
 - 8 S. Chen, Y. Hong, Y. Liu, J. Liu, C. W. T. Leung, M. Li, R. T. K. Kwok, E. Zhao, J. W. Y. Lam, Y. Yu and B. Z. Tang, *J. Am. Chem. Soc.*, 2013, **135**, 4926-4929.
 - 9 Y. Yuan, R. T. K. Kwok, B. Z. Tang and B. Liu, *J. Am. Chem. Soc.*, 2014, **136**, 2546-2554.
 - 10 M. P. Aldred, C. Li, G. F. Zhang, W. L. Gong, A. D. Q. Li, Y. Dai, D. Ma and M. Q. Zhu, *J. Mater. Chem.*, 2012, **22**, 7515-7528.
 - 11 X. Liu, J. Jiao, X. Jiang, J. Li, Y. Cheng and C. Zhu, *J. Mater. Chem. C*, 2013, **1**, 4713-4719.
 - 12 R. Hu, J. L. Maldonado, M. Rodriguez, C. Deng, C. K. W. Jim, J. W. Y. Lam, M. M. F. Yuen, G. Ramos-Ortiz and B. Z. Tang, *J. Mater. Chem.*, 2012, **22**, 232-240.
 - 13 H. Tong, Y. Hong, Y. Dong, H. J. W. Y. Lam, Z. Li, Z. Guo, Z. Guo and B. Z. Tang, *Chem. Commun.*, 2006, 3705-3707.
 - 14 B. Z. Tang, X. Zhan, G. Yu, P. P. Sze Lee, Y. Liu and D. Zhu, *J. Mater. Chem.*, 2001, **11**, 2974-2978.
 - 15 X. Zhang, Z. Chi, B. Xu, L. Jiang, X. Zhou, Y. Zhang, S. Liu and J. Xu, *Chem. Commun.*, 2012, **48**, 10895-10897.
 - 16 H. J. Yen, C. J. Chen and G. S. Liou, *Chem. Commun.*, 2013, **49**, 630-632.
 - 17 P. Lu, J. W. Y. Lam, J. Liu, C. K. W. Jim, W. Yuan, C. Y. K. Chan, N. Xie, Q. Hu, K. K. L. Cheuk and B. Z. Tang, *Macromolecules*, 2011, **44**, 5977-5986.
 - 18 J. Liu, J. W. Y. Lam, C. K. W. Jim, J. C. Y. Ng, J. Shi, H. Su, K. F. Yeung, Y. Hong, M. Faisal, Y. Yu, K. S. Wong and B. Z. Tang, *Macromolecules*, 2010, **44**, 68-79.
 - 19 J. Shi, Y. Wu, S. Sun, B. Tong, J. Zhi and Y. Dong, *J. Polym. Sci., Part A: Polym. Chem.*, 2013, **51**, 229-240.
 - 20 C. K. W. Jim, J. W. Y. Lam, A. Qin, Z. Zhao, J. Liu, Y. Hong and B. Z. Tang, *Macromol. Rapid Commun.*, 2012, **33**, 568-572.
 - 21 J. Liu, Y. Zhong, P. Lu, Y. Hong, J. W. Y. Lam, M. Faisal, Y. Yu, K. S. Wong and B. Z. Tang, *Polym. Chem.*, 2010, **1**, 426-429.
 - 22 J. Liu, Y. Zhong, J. W. Y. Lam, P. Lu, Y. Hong, Y. Yu, Y. Yue, M. Faisal, H. H. Y. Sung, I. D. Williams, K. S. Wong and B. Z. Tang, *Macromolecules*, 2010, **43**, 4921-4936.
 - 23 H. Li, H. Wu, E. Zhao, J. Li, J. Z. Sun, A. Qin and B. Z. Tang, *Macromolecules*, 2013, **46**, 3907-3914.
 - 24 W. Zhao, C. Li, B. Liu, X. Wang, P. Li, Y. Wang, C. Wu, C. Yao, T. Tang, X. Liu and D. Cui, *Macromolecules*, 2014, **47**, 5586-5594.
 - 25 P. Theato, *Angew. Chem., Int. Ed.*, 2011, **50**, 5804-5806.
 - 26 P. Y. Gu, C. J. Lu, Q. F. Xu, G. J. Ye, W. Q. Chen, X. M. Duan, L. H. Wang and J. M. Lu, *J. Polym. Sci., Part A: Polym. Chem.*, 2012, **50**, 480-487.
 - 27 L. Tang, J. K. Jin, A. Qin, W. Zhang Yuan, Y. Mao, J. Mei, J. Zhi Sun and B. Zhong Tang, *Chem. Commun.*, 2009, 4974-4976.
 - 28 H. Lu, F. Su, Q. Mei, X. Zhou, Y. Tian, W. Tian, R. H. Johnson and D. R. Meldrum, *J. Polym. Sci., Part A: Polym. Chem.*, 2012, **50**, 890-899.
 - 29 H. Lu, F. Su, Q. Mei, Y. Tian, W. Tian, R. H. Johnson and D. R. Meldrum, *J. Mater. Chem.*, 2012, **22**, 9890-9900.
 - 30 X. Zhang, X. Zhang, B. Yang, M. Liu, W. Liu, Y. Chen and Y. Wei, *Polym. Chem.*, 2014, **5**, 399-404.
 - 31 P. Y. Gu, C. J. Lu, Z. J. Hu, N. J. Li, T. t. Zhao, Q. F. Xu, Q. H. Xu, J. D. Zhang and J. M. Lu, *J. Mater. Chem. C*, 2013, **1**, 2599-2606.
 - 32 J. I. Chen and W. C. Wu, *Macromol. Biosci.*, 2013, **13**, 623-632.
 - 33 P. Y. Gu, C. J. Lu, F. L. Ye, J. F. Ge, Q. F. Xu, Z. J. Hu, N. J. Li and J. M. Lu, *Chem. Commun.*, 2012, **48**, 10234-10236.
 - 34 X. Shen, Y. Shi, B. Peng, K. Li, J. Xiang, G. Zhang, Z. Liu, Y. Chen and D. Zhang, *Macromol. Biosci.*, 2012, **12**, 1583-1590.
 - 35 X. Zhang, X. Zhang, B. Yang, M. Liu, W. Liu, Y. Chen and Y. Wei, *Polym. Chem.*, 2014, **5**, 356-360.
 - 36 X. Zhang, X. Zhang, B. Yang, J. Hui, M. Liu, Z. Chi, S. Liu, J. Xu and Y. Wei, *Polym. Chem.*, 2014, **5**, 683-688.
 - 37 X. Zhang, M. Liu, B. Yang, X. Zhang, Z. Chi, S. Liu, J. Xu and Y. Wei, *Polym. Chem.*, 2013, **4**, 5060-5064.
 - 38 H. Y. Li, X. Q. Zhang, X. Y. Zhang, B. Yang, Y. Yang, Z. F. Huang and Y. Wei, *Rsc Adv.*, 2014, **4**, 21588-21592.
 - 39 H. Y. Li, X. Q. Zhang, X. Y. Zhang, B. Yang, Y. Yang and Y. Wei, *Polym. Chem.*, 2014, **5**, 3758-3762.
 - 40 C. W. Bielawski and R. H. Grubbs, *Prog. Polym. Sci.*, 2007, **32**, 1-29.
 - 41 K. Zhang, J. Cui, M. Lackey and G. N. Tew, *Macromolecules*, 2010, **43**, 10246-10252.
 - 42 L. Ren, J. Zhang, C. G. Hardy, S. Ma and C. Tang, *Macromol. Rapid Commun.*, 2012, **33**, 510-516.
 - 43 J. A. Love, J. P. Morgan, T. M. Trnka and R. H. Grubbs, *Angew. Chem., Int. Ed.*, 2002, **41**, 4035-4037.
 - 44 L. F. Zhang, A. Eisenberg, *J. Am. Chem. Soc.*, 1996, **118**, 3618-3181.
 - 45 Y. S. Yu, L. F. Zhang, A. Eisenberg, *Macromolecules*, 1998, **31**, 1144-1154.
 - 46 A. Blanz, S. P. Armes, A. J. Ryan, *Macromol. Rapid Comm.*, 2009, **30**, 267-277.

Table of Contents:

Aggregation-Induced Emission Block Copolymers Based on Ring-Opening Metathesis Polymerization

*Yuming Zhao, Ying Wu, Guowei Yan, Ke Zhang **

AIE amphiphilic block copolymers were developed from ROMP for the first time. By self-assembly in selective solvents, water soluble fluorescent nano-objects were prepared with varied structures including micelles and vesicles.

